

The use of accumulation elements with lumped parameters to model the operation of heat exchange installations under randomly changing temperatures

Jacek Kropiwnicki^a, Bartosz Dawidowicz^{a*}, Przemysław Wojewódka^b, Andrzej Rogala^b

^aGdansk University of Technology, Faculty of Mechanical Engineering and Ship Technology, Narutowicza 11/12, 80-223, Gdansk, Poland, jacek.kropiwnicki@pg.edu.pl, bartosz.dawidowicz@pg.edu.pl

^bGdansk University of Technology, Faculty of Chemistry, Narutowicza 11/12, 80-223 Gdansk, Poland, andrzej.rogala@pg.edu.pl

*Corresponding author: e-mail: Bartosz Dawidowicz, bartosz.dawidowicz@pg.edu.pl

Abstract: At the design stage of heat exchange installation used for gas conversion it is required to test the stability of the installation operation for the expected variable heat loads. For this purpose, a numerical model of the installation can be used. The paper presents an original concept of modelling the operation of heat exchange installations for randomly changing temperatures. Accumulation elements with lumped parameters were used in the model, which significantly facilitates the definition of model parameters and the calculation itself at the design stage. Due to the randomly changing temperatures supplying the accumulation element by the heating medium and the non-linear nature of the functions used in the calculation model, the iterative procedure was used for calculations. The process of validation of the proposed computational model of the accumulation element with lumped parameters was carried out for a water installation powered by a natural gas-fired boiler. The obtained results showed very good accuracy of the applied approach, the root mean square error for tested data has reached 1°C to 3°C, depending on the analysed case.

Keywords: heat transfer modelling; warming-up process; chemical installation temperature control; randomly modified conditions

This article has been accepted for publication and undergone full peer review but has not been through the copyediting, typesetting, pagination and proofreading process which may lead to differences between this version and the version of record. Please cite this article as DOI: [10.24425/cpe.2024.149461](https://doi.org/10.24425/cpe.2024.149461).

Received: 21 December 2023 | Revised: 15 May 2024 | Accepted: 28 May 2024



1. INTRODUCTION

Waste heat recovery is playing more and more important roles in industrial energy systems (Gao et al., 2019; Kang et al., 2019) such as in processes of chemical engineering, petroleum engineering (Shu et al., 2020), metallurgy engineering (Jiang et al., 2019), solar energy engineering (Han et al. 2020) and nuclear engineering (Kluba and Field 2019). Thus, efficient heat transfer has become increasingly important for the green transition and the replacement of fossil fuels with renewable energy sources. Heat exchangers and flow control of the medium in a process, as a critical component of any thermal system, play a critical role in the efficient and safe operation of the flow heating systems as a means of providing effective and suitable heat transfer for cooling, heating, material phasing change, depending on the industry and needs and even in thermal control system for spacecraft (Zheng and Zhao, 2022a; Zheng and Zhao, 2022b). For example the combination of waste heat of at recovery and methanol steam reforming is beneficial to the development of hydrogen production and other synthetic fuels. Thus, in terms of the correct functioning of the above-mentioned installations, it is important to ensure the effective cooperation of the heat and mass transport elements with the regulating elements (ElAzab et al., 2018; Skoglund et al., 2006; Dehghan and Barzegar, 2011). As shown by simulation studies (Kamal et al., 2019), the optimization of the energy system was able to achieve an annual cost reduction of 10–17%. The quality of cooperation can be determined by numerical simulation, using efficient models and a flexible interface (Dahash et al., 2019; Li et al., 2019; Kuang et al., 2018) enabling the correct implementation of the installation into the computing environment, as well as definition of boundary and initial conditions (Giraud et al., 2017; Li et al., 2017; Oppelt et al., 2016). Modelled heat exchange systems can be divided into control elements related to other heat transport mechanisms, e.g., in a proton exchange membrane fuel cell, the first control element is an anode and a cathode, while the second control element is the liquid in the cooling channels (Bird and Jain, 2020). In the case of elements joining or dividing heat fluxes, it is assumed that these elements are well insulated and heat losses can be neglected. On the other hand, the fluid temperature and mass flow rate at the outlet are calculated on the basis of the first law of energy balance and the conservation of mass (Barone et al., 2020; Bird and Jain, 2020). The propagation of water in pipes can be modelled by considering the inlet and outlet of a pipe and calculating the output based on the propagation delay (Gabrielaitiene et al., 2007; Vesterlund and Dahl, 2015).

Wide and complex process models and the cross-interconnection of modelled variables makes the modelling work more difficult and challenging. Especially the determination and tuning of the parameters of complex models are often laborious and time-consuming. In the papers

(Zheng and Zhao, 2022a; Zheng and Zhao, 2022b) the dynamic flow allocation of the parallel heat exchanger system in spacecraft has been researched. The optimal control problem was transformed into a nonlinear programming problem that has been solved by PSO and SQP with an exact external penalty function, respectively, by the CVP method and time-scaling method. Through these modeling and algorithm construction methods, the accurate gradient of the optimization problem could be obtained and used in the solving algorithm. The simulation results showed that the EPSQP algorithm successfully solved the optimization problem with the temperature path constraint. While in the paper (Kropiwnicki et al., 2021) presents a new method for modelling the warming-up process of a water system with elements regulating the flow in a stochastic manner. It presents the basic equations describing the work of typical elements which the water installation is composed of. The installation is used to control the temperature of chemical reactors which can be used in petrochemical processes like methanol synthesis and synthetic gas production (Wysocka et al., 2019). In commonly used methods, the modelling of the warming-up process of such systems is performed by solving the conservation equations describing the operation of individual elements of the installation, with clearly defined boundary conditions. Proposed in the method, a new computational algorithm was used in the form of an iterative procedure, enabling the use of boundary conditions that can be stochastically modified during the warming-up process. This solution can be used to facilitate and accelerate calculations and simulation work.

As presented in the paper by Bhutta et al. (2012) the optimal design of heat exchangers using methods such as the logarithmic mean temperature difference (LMTD) method and the Efficiency-number of Heat-transfer Units (η -NTU) method is costly and time-consuming (Bhutta et al., 2012). Studies by many researchers have shown that simulations of various types of heat exchangers using CFD are reliable (Pal et al., 2016; Wang et al., 2021). Therefore, CFD numerical simulations can minimize unnecessary test work and provide great convenience for efficient optimal design of heat exchangers. Generally, numerical simulation results need to be combined with optimization algorithms to obtain the optimal solution. As shown by the research of Yusuf et al. (2021) the Pareto optimal solution set of NSGA-II using TOPSIS can be used to optimize the parameters of the hybrid system to obtain the optimum performance of the system operating at maximum power point. Li et al. (2022) in the paper carried out a multi-objective optimization, based on computational fluid dynamics (CFD) and non-dominated sequencing genetic algorithm (NSGA-II) for the optimal performance of a plate-fin heat exchanger for hybrid vehicle engine. Support vector machine regression (SVR) was used to establish the objective function, and the NSGA-II algorithm was adopted to obtain the Pareto optimal

solution set. Finally, the optimal solution was evaluated comprehensively by using TOPSIS. The non-dominated sequencing genetic algorithm (NSGA-II) is widely used for optimization design due to its advantages such as fast operation and good convergence of the solution set. Thus, the current studies primary aim is multi-objective optimization performed using CFD and artificial intelligence. With the fast pace of computational technologies, the use of AI is ever-increasing, and artificial neural networks (ANN) are invariably applied to perceive and predict patterns in complex systems (Shi et al., 2019). Genetic algorithms inspired by natural selection can accompany ANNs while the latter predict the system's output; the former can reveal a system's optimized state (Aminmahalati et al., 2021; Zhou et al., 2004). An obvious advantage of genetic algorithms is the ability to optimize multi objectives simultaneously. Genetic algorithms can be combined with CFD models, too, as chromosomes defined in the genetic algorithms can replace the input parameters.

The paper presents an original method of modeling the operation of a heat exchange installation in conditions of random variable temperatures. Such variable operating conditions are typical for thermal-flow and process installations that use power sources with variable parameters, e.g. a natural gas to dimethyl ether conversion installation powered from a small hydrocarbon deposits.

Natural gas conversion to dimethyl ether requires a multi-operational process plant divided into specialized sub-units, responsible for subsequent stages of the process. The main sub-units of the plant are as follows, in order of process progression: Combustion Unit, Reforming Unit, Synthesis Unit, Amine Treatment Unit and Water Treatment Unit. In each of them, several heat exchange stages take place, with process temperature as one of the major factors affecting the efficiency of the process plant. To secure the plant demand for heat and cold streams, two auxiliary units are indispensable for the process proper operation: Heating Unit and Cooling Unit. Proper design of the auxiliary heating and cooling units requires prediction of the heat exchange in each of the main process units in dependency of the external, variable parameters – natural gas flow rate depending on the nature and level of exploitation of the field and the ambient temperature deviations (Sobczak et al., 2022).

The combustion unit is the first stage in the process of conversion of natural gas (CH_4) to DME. After combustion, the exhaust stream that is composed of CO_2 , N_2 , O_2 and traces of NO_x enters the absorption tower to separate the CO_2 from other gases. The absorption process utilizes amine solution, and its absorption capacity is highly dependent on the solution temperature. After the separation, the CO_2 -rich amine is heated up to desorb the CO_2 and utilize it in the next stage. With variable combustion process conditions (effecting variable enthalpy of exhaust

stream directed to amine) and changing ambient conditions, the amine solution temperature can be greatly affected and in consequence the amount of absorbed and desorbed CO₂ can change over time, affecting the next stage – Reforming Unit – which operates on strict molar ratio of CO₂ to CH₄ to generate the synthesis gas and any disturbances of this ratio can affect greatly the efficiency of the whole plant or even stop its operation. This entails the high importance of proper temperature control in previously described absorption and desorption processes and brings additional requirements for the design stage of heating and cooling systems, to test their ability for response for the change of external parameters to secure the stable process operation (Brown et al., 1991).

During the design stage of every process plant, special attention is given to the start-up and shutdown stage. On the contrary to the normal operation stage, where all the processes are assumed as steady state and are affected only by the external variable fluctuations, the start-up and shutdown periods are described as transient states, where much more factors affect the process progression, including but not limited to geometrical aspects of the process equipment, heating (or cooling) the equipment, pressure build-up and fluctuations, temperature fluctuations, heat demand change due to reaction enthalpy effect. Mathematical description of these stages is a great challenge for designers, even with modelling and simulation tools. The use of the computational model of the accumulation element with lumped parameters can greatly improve the simulation result of the heat exchange units in the designed plant but also in optimization processes of already built units (Alsanousie et al., 2021).

This work presents an original concept of modelling the operation of heat exchange installations for randomly changing temperatures. The described method uses a model with lumped characteristics to facilitate the simulation of the system operation at the stage of initial system design without the need for full technical specifications of individual elements. When integrating the operation of thermal and process components, there is little probability that all elements will be specified at the same time, especially when some of them have to be chosen from those available on the market.

2. ACCUMULATION ELEMENT WITH LUMPED PARAMETERS

2.1 Computational model

One of the key parts of a heat exchange installation operating in conditions of randomly changing temperatures is the accumulation element, which enables the storage of heat and its

subsequent release, stabilizing the operating parameters of the installation. One of the special kinds of accumulative elements is a heat accumulator, which is usually filled with a medium with a higher temperature, while emptying it with a medium with a lower temperature, in order to store thermal energy. This process is accompanied by the accumulation of heat in the walls of the tank and the transfer of heat from the walls to the environment, which is usually the surrounding air. In the case of variable heat loads, the accumulation element is also a heat exchanger, which can be considered as a general case of the accumulation element. In a situation where only the heat accumulator is considered, it can be treated as a heat exchanger with a cold medium (receiving heat) in the form of ambient air at a constant temperature. In the presented method, it was assumed that the accumulation elements in the heat exchanger are the following factors: the hot fluid, the cold fluid, and the exchanger wall. In order to shorten the calculation time and reduce the number of heat exchanger design parameters required for the simulation, it was decided to use a model with lumped parameters. This means that in the storage element under consideration, and in the general case in the heat exchanger, the structure of the exchanger is a single heat storage element, the parameters of which can be determined by one mass, temperature, specific heat, etc. Similarly, the cold and hot medium are a single heat storage element. In general, the accumulation element consists of three masses: the structure of the heat exchanger, the hot medium and the cold medium.

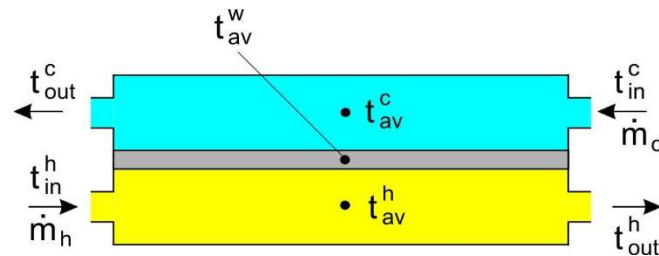


Figure 1. Shows a diagram of the heat exchanger as an accumulation element with lumped parameters.

For the system shown in Figure 1, three equations describing the energy balance can be assumed, neglecting the losses to the environment. The process of energy accumulation in the heating medium is described by the following equation:

$$Q_{in}^h = Q_{acc}^h + Q_{\alpha}^h + Q_{out}^h \quad (1)$$

where Q_{in}^h - heat flux delivered by the heating medium, Q_{acc}^h - heat accumulated in the heating medium, Q_{α}^h - heat flux transferred between the heating medium and the wall, Q_{out}^h - heat flux discharged by the heating medium. It was assumed that the entire mass of the heat exchanger structure is concentrated in a single element and it takes a form of a plane wall. The process of

energy accumulation in the heat exchanger wall (heat exchanger structure) is described by the following equation:

$$Q_{\alpha}^h = Q_{acc}^w + Q_{\alpha}^c \quad (2)$$

where Q_{acc}^w - heat accumulated in the heat exchanger wall, Q_{α}^c - heat flux transferred between the wall and the cooling medium. The process of energy accumulation in the cooling medium is described by the following equation:

$$Q_{in}^c + Q_{\alpha}^c = Q_{acc}^c + Q_{out}^c \quad (3)$$

where Q_{in}^c - heat flux delivered by the cooling medium, Q_{acc}^c - heat accumulated in the cooling medium, Q_{out}^c - heat flux discharged by the cooling medium.

The components of Equations (1)–(3) are defined below:

$$Q_{in}^h = \dot{m}_h \cdot c_h \cdot (t_{in}^h - t_{ref}) \quad (4)$$

where \dot{m}_h is mass flow rate of the heating medium in the heat exchanger, c_h is specific heat of the heating medium, t_{in}^h is inlet temperature of the heating medium, t_{ref} is reference temperature,

$$Q_{in}^h = \dot{m}_h \cdot c_h \cdot t_{in}^h - \dot{m}_h \cdot c_h \cdot t_{ref} \quad (5)$$

Assuming that:

$$t_{ref} = 0 \quad (6)$$

we obtain:

$$Q_{in}^h = \dot{m}_h \cdot c_h \cdot t_{in}^h \quad (7)$$

Having the same reference temperature for all considered cases ($t_{ref} = 0$), it can be assumed analogically:

$$Q_{out}^h = \dot{m}_h \cdot c_h \cdot t_{out}^h \quad (8)$$

where t_{out}^h is outlet temperature of the heating medium,

$$Q_{acc}^h = m_h \cdot c_h \cdot (\Delta t_{av}^h / \Delta \tau) \quad (9)$$

where m_h is the mass of the heating medium in the heat exchanger, Δt_{av}^h is a change of the average temperature of the heating medium over the computational time step $\Delta \tau$. It was assumed that the change of the average temperature of the heating medium over time $\Delta \tau$ can be determined using the following equation:

$$\Delta t_{av}^h = t_{av_end}^h - t_{av_ini}^h \quad (10)$$

where $t_{av_ini}^h$ is the average temperature of the heating medium in the heat exchanger during the previous computational step (*ini*), and $t_{av_end}^h$ is the average temperature of the heating medium in the heat exchanger in the current computational step (*end*):

$$t_{av_ini}^h = \frac{t_{in}^h(\tau-\Delta\tau) + t_{out}^h(\tau-\Delta\tau)}{2} \quad (11)$$

where τ is a current time of the process,

$$t_{av_end}^h = \frac{t_{in}^h(\tau) + t_{out}^h(\tau)}{2} \quad (12)$$

By the discretization of the process, the current time of the process can be replaced by a computational step (k):

$$\tau(k) - \tau(k-1) = \Delta\tau \quad \text{for } k > 1 \quad (13)$$

The average temperature of the heating medium in the heat exchanger in the previous ($k-1$) and current (k) computational steps can be then defined as follows:

$$t_{av_ini}^h = \frac{t_{in}^h(k-1) + t_{out}^h(k-1)}{2} \quad (14)$$

$$t_{av_end}^h = \frac{t_{in}^h(k) + t_{out}^h(k)}{2} \quad (15)$$

Analogously for the cooling medium:

$$Q_{in}^c = \dot{m}_c \cdot c_c \cdot t_{in}^c \quad (16)$$

where \dot{m}_c is mass flow rate of the cooling medium in the heat exchanger, c_c is specific heat of the cooling medium, t_{in}^c is inlet temperature of the cooling medium,

$$Q_{out}^c = \dot{m}_c \cdot c_c \cdot t_{out}^c \quad (17)$$

where t_{out}^c is outlet temperature of the cooling medium,

$$Q_{acc}^c = m_c \cdot c_c \cdot (\Delta t_{av}^c / \Delta\tau) \quad (18)$$

where m_c is the mass of the cooling medium in the heat exchanger, Δt_{av}^c is a change of the average temperature of the cooling medium over the computational time step $\Delta\tau$,

$$\Delta t_{av}^c = t_{av_end}^c - t_{av_ini}^c \quad (19)$$

where $t_{av_ini}^c$ is the average temperature of the cooling medium in the heat exchanger during the previous computational step (*ini*), and $t_{av_end}^c$ is the average temperature of the cooling medium in the heat exchanger in the current computational step (*end*):

$$t_{av_ini}^c = \frac{t_{in}^c(\tau-\Delta\tau) + t_{out}^c(\tau-\Delta\tau)}{2} \quad (20)$$

$$t_{av_end}^c = \frac{t_{in}^c(\tau) + t_{out}^c(\tau)}{2} \quad (21)$$

The average temperature of the cooling medium in the heat exchanger in the previous ($k-1$) and current (k) computational steps can be then defined as follows:

$$t_{av_ini}^c = \frac{t_{in}^c(k-1) + t_{out}^c(k-1)}{2} \quad (22)$$

$$t_{av_end}^c = \frac{t_{in}^c(k) + t_{out}^c(k)}{2} \quad (23)$$

It was assumed that the entire mass of the heat exchanger structure is concentrated in a single element, which simplifies calculation of the heat accumulated in it:

$$Q_{acc}^w = m_w \cdot c_w \cdot (\Delta t_{av}^w / \Delta \tau) \quad (24)$$

where m_w is the mass of the wall, c_w is the specific heat of the wall, Δt_{av}^w is a change of the average temperature of the wall over the computational time step $\Delta \tau$,

$$\Delta t_{av}^w = t_{av_end}^w - t_{av_ini}^w \quad (25)$$

where $t_{av_ini}^w$ is the average temperature of the wall during the previous computational step (*ini*), and $t_{av_end}^w$ is the average temperature of the wall in the current computational step (*end*):

$$t_{av_ini}^w = t_w(\tau - \Delta \tau) \quad (26)$$

$$t_{av_end}^w = t_w(\tau) \quad (27)$$

The average temperature of the wall in the previous ($k-1$) and current (k) computational steps can be then defined as follows:

$$t_{av_ini}^w = t_w(k-1) \quad (28)$$

$$t_{av_end}^w = t_w(k) \quad (29)$$

The heat flux transferred between the heating medium and the wall can be calculated as follows:

$$Q_{\alpha}^h = \alpha_h \cdot A \cdot \Delta t_{h_w} \quad (30)$$

where α_h is the heat transfer coefficient for the heating medium, A is the heat transfer surface, Δt_{h_w} is the temperature difference between the heating medium and the wall:

$$\Delta t_{h_w} = t_{av_end}^h - t_{av_end}^w \quad (31)$$

The heat flux transferred between the wall and the cooling medium can be calculated as follows:

$$Q_{\alpha}^c = \alpha_c \cdot A \cdot \Delta t_{w_c} \quad (32)$$

where α_c is the heat transfer coefficient for the cooling medium, Δt_{w_c} is the temperature difference between the wall and the cooling medium:

$$\Delta t_{w_c} = t_{av_end}^w - t_{av_end}^c \quad (33)$$

2.2 Boundary conditions

In order to calculate the average values of the hot (Eq. 15) and cold (Eq. 23) medium, it is necessary to determine the temperature of the medium at the inlet (in) and outlet (out) of the heat exchanger, which are the boundary conditions for the considered element. The calculation model assumes that the average medium temperature is equal to the arithmetic mean of the inlet and outlet temperatures. The use of this simplification can be applied, when static conditions are implemented. Technically, this means that the temperature of the fluid in the heat exchanger varies linearly with respect to length. Unfortunately, for dynamic conditions, such an

assumption cannot be made. For example, when the system is started up, the temperature throughout the heat exchanger is equal to the ambient temperature, and there is a step change of temperature at the inlet. This situation absolutely does not correspond to the expected linear distribution of the temperature. It has been proposed, that the temperature at the inlet to the heat exchanger should be corrected, taking into account the refilling the chamber of the heat exchanger with a medium of changed temperature. It was assumed that when the refilling process is finished, the changed boundary conditions cover the entire heat exchanger.

A chamber refilling time for heating medium can be calculated using following equation:

$$\tau_{ch}^h = \frac{\rho_{ch}^h \cdot V_{ch}^h}{\dot{m}_{ch}^h} \quad (34)$$

where τ_{ch}^h is time of refilling a chamber of heating medium, ρ_{ch}^h is the average density of the heating medium in the chamber, V_{ch}^h is the volume of the heating chamber, and \dot{m}_{ch}^h is the mass flow rate of the heating medium. However, the chamber refilling time can be calculated as the number of computational steps that will elapse between the triggering of the impulse at the inlet to the chamber and the impulse reaching the outlet from the chamber:

$$k_{ch}^h = \text{round} \left(\frac{\tau_{ch}^h}{\Delta\tau} \right) \quad (35)$$

Finally, the inlet temperature of the heating medium for computational step (k) can be calculated as follows:

$$t_{in}^h(k) = t_{sup}^h(0) \quad \text{for} \quad k \leq k_{ch}^h \quad (36)$$

$$t_{in}^h(k) = t_{sup}^h(k - k_{ch}^h) \quad \text{for} \quad k > k_{ch}^h \quad k > k_{ch}^h \quad (37)$$

where t_{sup}^h is the supply temperature of the heating medium delivered by the pipe system.

Analogously for the cooling medium a chamber refilling time for cooling medium can be calculated using the following equation:

$$\tau_{ch}^c = \frac{\rho_{ch}^c \cdot V_{ch}^c}{\dot{m}_{ch}^c} \quad (38)$$

where ρ_{ch}^c is the average density of the cooling medium in the chamber, V_{ch}^c is the volume of the cooling chamber, and \dot{m}_{ch}^c is the mass flow rate of the cooling medium. A chamber refilling computational steps can be calculated as follows:

$$k_{ch}^c = \text{round} \left(\frac{\tau_{ch}^c}{\Delta\tau} \right) \quad (39)$$

The inlet temperature of the cooling medium for computational step (k) can be calculated as follows:

$$t_{in}^c(k) = t_{sup}^c(0) \quad \text{for} \quad k \leq k_{ch}^c \quad (40)$$

$$t_{in}^c(k) = t_{sup}^c(k - k_{ch}^c) \quad \text{for} \quad k > k_{ch}^c \quad (41)$$

where t_{sup}^c is the supply temperature of the cooling medium delivered by the pipe system.

2.3 Iterative calculation procedure of the accumulation element

Calculation of the accumulation element, which in general can take the form of a heat exchanger, requires defining the parameters of the modelled element (Section 2.1) and boundary conditions (Section 2.2). Then it is necessary to solve the set of Equations (1)–(3) in order to calculate the temperatures of the hot (t_{out}^h) and cold (t_{out}^c) medium at the exit of the heat exchanger and the wall temperature of the heat exchanger (t_w). According to Equations (28) and (29), the temperature $t_w(k)$ is the average wall temperature for the calculation step (k), the current one, while $t_w(k - 1)$ is the average wall temperature for the previous calculation step.

Due to the assumed random-variable nature of the temperature supplying the heat exchanger with the hot (t_{sup}^h) and cold (t_{sup}^c) medium and the non-linear nature of the functions used in the calculation model, the iterative calculation procedure (Knabner and Angermann, 2003) of the accumulation element was used in the calculations. Fig. 2 shows the iterative procedure for calculating the accumulation element. The procedure consists of three sections. In the first one (data import section) data of modelled objects are entered and the number of computational steps corresponding to chamber refilling time are calculated. In the second section (time delay section), the temperature of the heating and cooling factors are calculated on the supply to the storage element chambers. In the last section (accumulation and heat exchange section) the temperature of the factors at the exit from the accumulation element and the average temperature of the wall separating the heating and cooling fluid are calculated using the iterative method. After completing the calculations in the third section, the condition is checked whether the simulation end time has been reached ($k = k_{max}$). If not, the calculations are carried out for the next step and time increased by the period $\Delta\tau$.

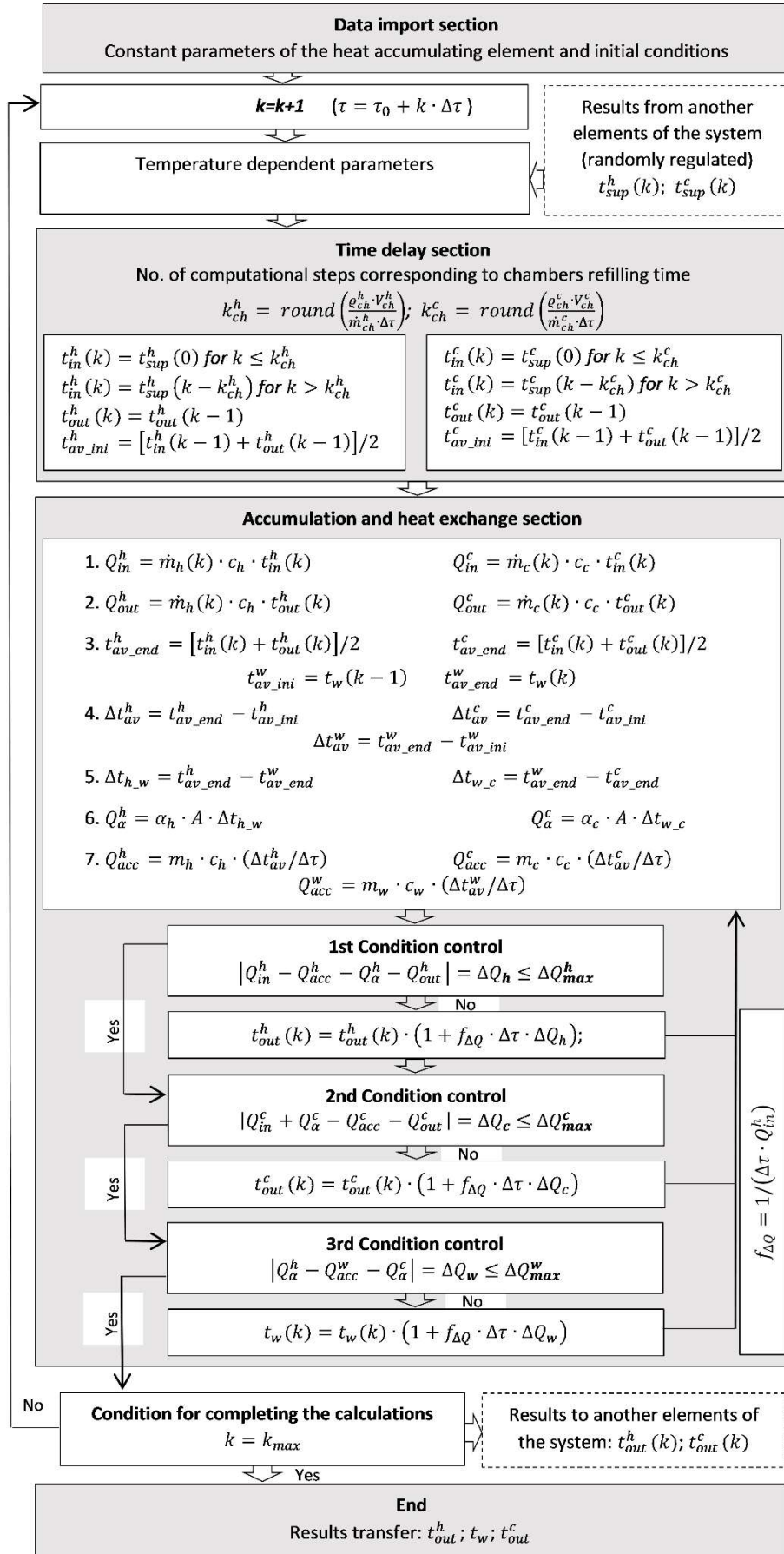


Figure 2. Iterative calculation procedure of the accumulation element.

The calculation procedure of the accumulation element enables simulation of the operation of the considered element of the installation for the indicated period of time, while for practical reasons the time step has been replaced with the calculation step in accordance with the following relationship:

$$\tau = \tau_0 + k \cdot \Delta\tau \quad (42)$$

The procedure includes, in addition to the condition that ends the calculations, when the end of the considered simulation time $k = k_{max}$, is reached, also three convergence conditions allowing to control the fulfillment of energy balances in the hot, cold fluid and wall. If any of the above conditions is not met, the internal calculation loop is repeated after correcting the appropriate temperature. The result of the calculations are tables of temperatures t_{out}^h ; t_w ; t_{out}^c for the considered range of calculation steps.

The sought temperatures (t_w , t_{out}^c , t_{out}^h) are calculated by solving the set of Equations (1)–(3). Due to randomly changing temperatures, the iterative procedure presented in Fig. 2 was used to solve this set of equations. The solution is obtained by successive approximations of the temperatures sought. However, in accordance with the adopted model, these values are adjusted in the next iteration step in accordance with the formulas presented in Fig. 2, so that conditions 1, 2 and 3 are finally met simultaneously. These conditions result directly from the balance equations (1)–(3) and allow to check whether they are met.

3. VALIDATION OF THE COMPUTATIONAL MODEL

The process of validation of the proposed computational model of the accumulation element with lumped parameters was carried out for the water installation, the diagram of which is shown in Fig. 3. The main parameters of the elements of the tested installation are presented in Tab. 1. Heat transfer coefficients for the cooling and heating medium were calculated using H. Hausen correlation formula (Pudlik, 2012). The analysed system consists of a boiler (BO), in which the water of the hot circuit is heated to the temperature T_{out}^b , then the water is supplied to the heat accumulator (A_{cc}) via the R1 pipeline. This element is the first of the elements considered during the validation of the computational model of the accumulation element with lumped parameters. At the entrance to the heat accumulator, the T_{acc} temperature is measured. In order to standardize the method of declaring parameters, the heat accumulator was treated as a heat exchanger, with surrounding air used as the cooling medium. In order to meet the formal requirements of the calculation procedure for the heat exchanger, it was assumed that the volume of the chamber through which the coolant (air) flows is equal to the volume of the chamber with the heating medium, while the mass flow rate was selected as 100 times greater

than the mass flow of the heating medium. As a result, the temperature increase of the cooling air was marginally small (below 0.1 K), which corresponds well to the regular operating conditions of well insulated accumulator. The R2 pipeline connects the heat accumulator with a three-way valve, which, depending on the setting, redirects the water flow through the R3 pipeline to the heat exchanger (HE) or to the R5 and R6 pipelines. The water flowing through the heat exchanger is cooled in it and then delivered to the R4 and R6 pipelines. The hot water temperature is measured before and after the heat exchanger, which is marked T^h_{in} and T^h_{out} respectively. The heat exchanger is the second element considered during the validation of the computational model of the accumulation element with lumped parameters. Pipeline R6 supplies water to the hot water circuit forcing pump, from which water is fed to the flow meter, and pipework R7, which supplies water to the boiler. At the water inlet to the boiler, the temperature (T^b_{in}) is also measured. In the heat exchanger element, the heat from the hot water is removed by the cold water, which is supplied from a large-capacity tank. The cold water temperature is measured before and after the heat exchanger, which is marked as T^c_{in} and T^c_{out} respectively. During the tests, the flow rate of hot and cold water was constant.

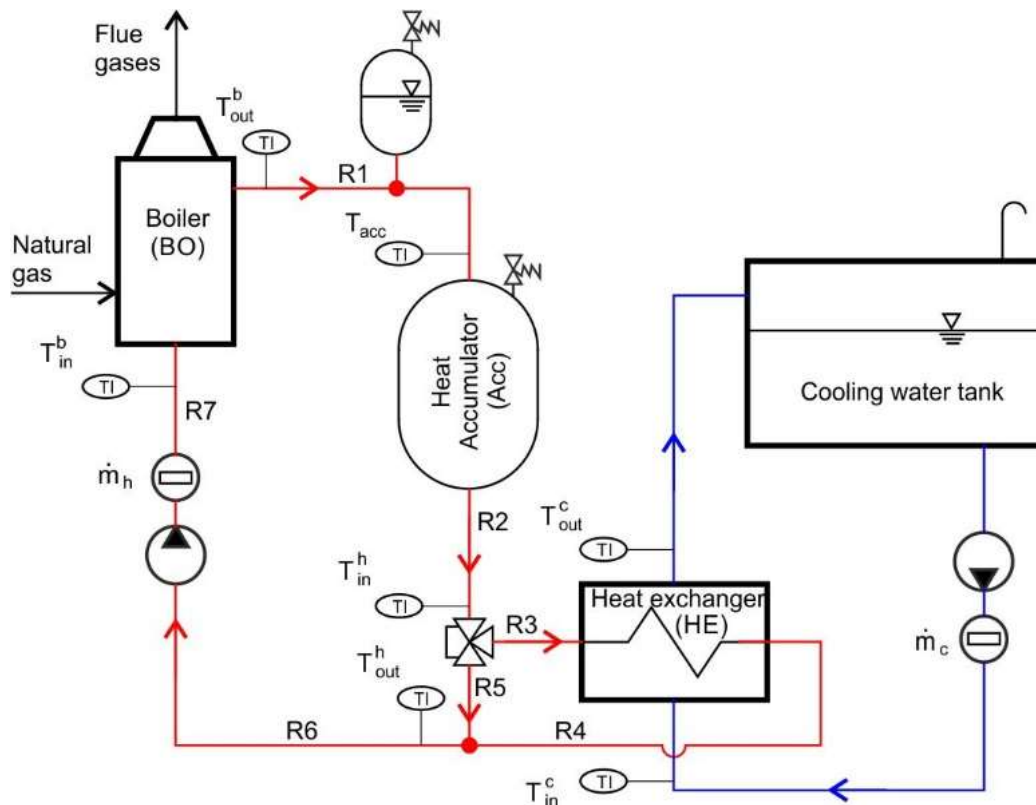


Figure 3. The scheme of the water installation used to validate the computational model of the accumulation element with lumped parameters.

The model assumes that the temperatures of the heating water and cooling water can be regulated randomly. The prepared model validation uses a system in which both mentioned temperatures can be subject to random changes. In addition, the system has a three-way valve that can randomly change the settings, although during validation there was no such action, because the threshold temperature was not exceeded. To better illustrate the sequence of calculations for individual system elements, an additional drawing (Fig. 4), containing a functional diagram of the analyzed system has been presented. The iterative method of solving the set of equations enables the use of non-linear equations, which makes the model relatively flexible.

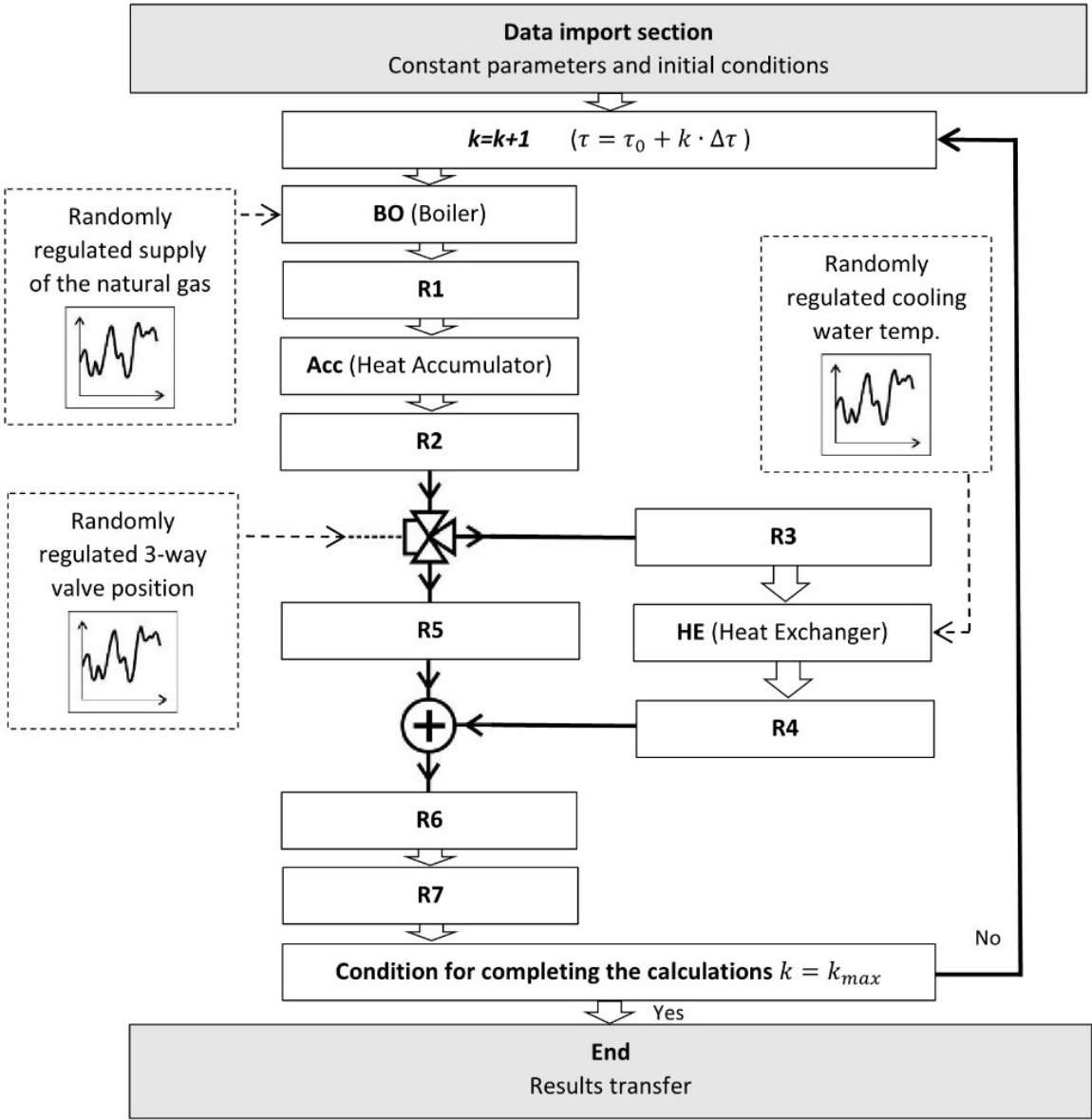


Figure 4. Functional diagram of the analysed system.

Table 1. Main parameters of the elements of the tested installation.

Parameter	HE	Acc	R1	R2	R3	R4	R5	R6	R7	BO
Mass flow rate (cooling) [kg/min]	3.50	426.9	-	-	-	-	-	-	-	-
Mass flow rate (heating) [kg/min]	4.27	4.27	4.27	4.27	4.27	4.27	0.00	4.27	4.27	4.27
Heat exchange area [m ²]	0.600	1.346	-	-	-	-	-	-	-	-
Volume of channel (cooling) [dm ³]	0.400	2.500	-	-	-	-	-	-	-	-
Mass of membrane (wall) [kg]	3.900	6.775	-	-	-	-	-	-	-	-
Volume of channel (heating) [dm ³]	0.400	2.500	0.371	0.183	0.020	0.019	0.023	0.260	0.093	0.343
Specific heat capacity (cooling) [J/(kg·K)]	4180	1006	-	-	-	-	-	-	-	-
Specific heat capacity (membrane) [J/(kg·K)]	478	478	-	-	-	-	-	-	-	-
Specific heat capacity (heating) [J/(kg·K)]	4180	4180	-	-	-	-	-	-	-	-

To simulate the operation of the installation shown in Fig. 3, the calculation model of the accumulation element with lumped parameters described in Section 2 was used. Individual elements of the installation highlighted in the diagram were considered as connected in series, so the calculation results for the previously placed element were input data for the next element. In the tests, the three-way valve was set in such a way that the flow of heating water was

bypassing the R5 pipeline, therefore the mass flow rate for this element was zero. It was assumed that the initial temperature of the heating and cooling fluid was the same throughout the installation and was the same as the temperature of the surrounding air (13 °C). After starting the boiler, the measured temperature of the fluid leaving this element (T_{out}^b) was treated as the set point in the simulation. Similarly, the measured temperature of the coolant supplying the heat exchanger (T_{in}^c) was treated as passed in the simulation. The courses of the set temperatures of the heating and cooling fluid are shown in Fig. 5. Simulations in individual elements of the installation were carried out using the iterative calculation procedure of the accumulation element presented in Fig. 2, with the exception that pipelines R1–R7 were calculated omitting heat exchange processes, due to the insulation of the pipelines and negligible heat loss to the environment. However, in the case of the Acc element, which had a relatively large heat exchange surface, the calculations assumed that the cooling factor was the surrounding air at a constant temperature. The simulation results are shown in Figs. 6–10.

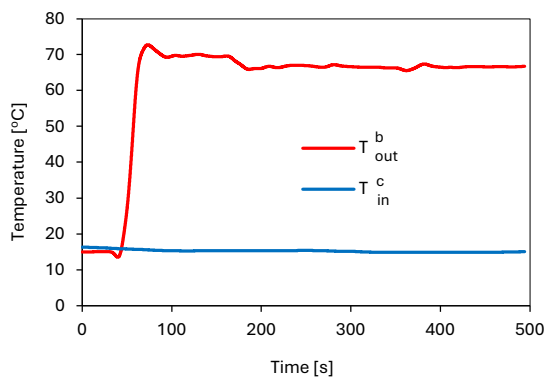


Figure 5. The set temperature of the heating fluid at the outlet of the boiler (T_{out}^b) and temperature of the cooling fluid at the inlet to the heat exchanger (T_{in}^c).

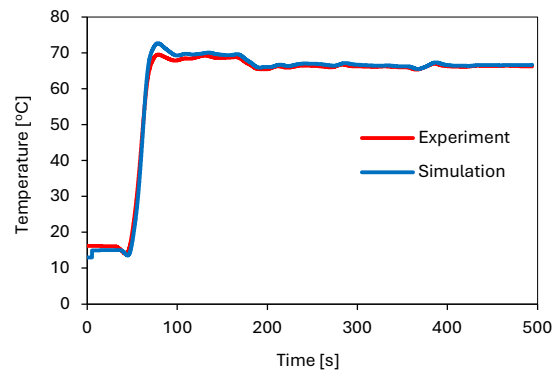


Figure 6. Comparison of the temperature of the heating fluid at the inlet to the heat accumulator obtained from the experiment (T_{acc}) and simulation.

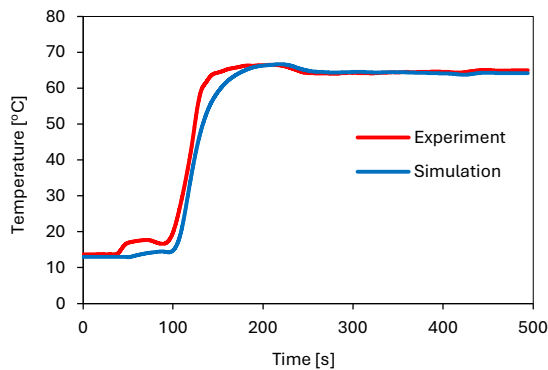


Figure 7. Comparison of the temperature of the heating fluid at the inlet to the heat

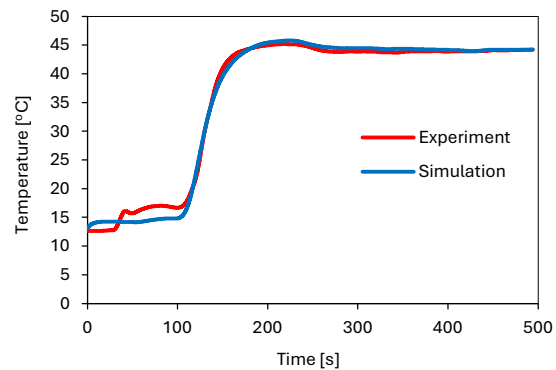


Figure 8. Comparison of the temperature of the heating fluid at the outlet of the heat

exchanger obtained from the experiment
(T_{in}^h) and the simulation.

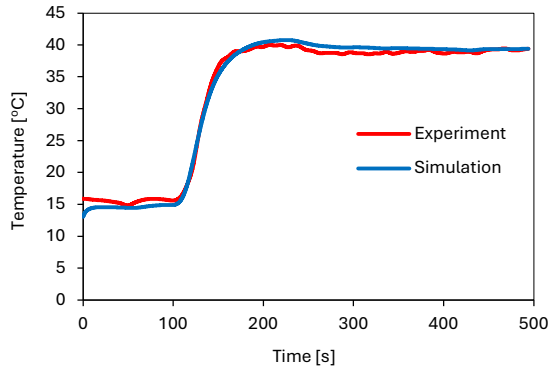


Figure 9. Comparison of the temperature of the coolant at the outlet of the heat exchanger obtained from the experiment (T_{out}^c) and the simulation.

exchanger obtained from the experiment
(T_{out}^h) and simulation.

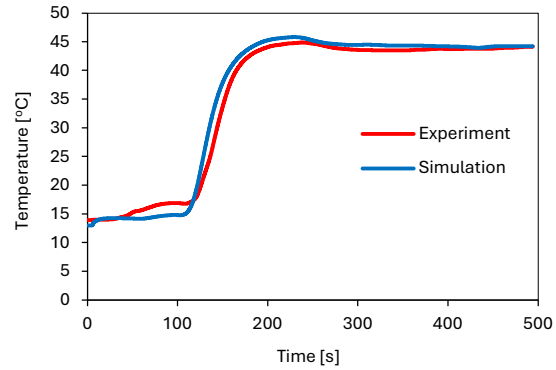


Figure 10. Comparison of the temperature of the heating fluid at the inlet to the boiler obtained from the experiment (T_{in}^h) and the simulation.

Due to the varied ambient conditions around the tested installation, at the beginning of the analysed heating process, slight differences in the level of the temperature set in the simulation of 13 °C and the actual temperature recorded in the experiment can be observed. After starting the boiler, the temperature of the heating water flowing to the system is successively increased until it reaches the set level (Fig. 5). Due to the very large capacity of the cooling water tank, the temperature of this medium is practically constant throughout the entire period of the test (Fig. 5). In the simulation, it was assumed that the pipelines connecting the individual elements of the installation were well insulated so that the heat exchange from the pipelines to the environment was negligible. The comparison of the simulation and experiment results shows that this assumption leads to small errors and the recorded temperature of the heating water supplying the heat accumulator is lower than that obtained from the simulation, especially in the highest temperature range (Fig. 6). In the other analysed nodes of the installation, there is good agreement between the temperatures recorded during the experiment and those obtained from the simulation (Figs. 6–10). In the last analysed node (Fig. 10), it can be observed that the delay of the temperature course coming from the simulation in relation to the experimental one, during the most rapid change, does not exceed 10 seconds.

Based on the obtained temperature courses, the mean square error of the temperature (RMSE) obtained from the experiment and simulation was determined according to the following equation:

$$RMSE = \sqrt{\frac{1}{k_{max}} \cdot \sum_{k=1}^{k_{max}} (t_k^{sym} - T_k^{exp})^2} \quad (43)$$

where:

k_{max} – number of points in the analysed series,

t_k^{sym} – calculated temperature,

T_k^{exp} – temperature measured in the experiment.

Tab. 2 shows the root-mean-square error for time series obtained from simulations and experimental tests at selected points of the installation shown in Fig. 3.

Table 2. Root-mean-square error analysis for selected points of the installation.

Point of the installation (reference temperature)	RMSE [°C]
Inlet of heating fluid to the heat accumulator (T_{acc})	1.1
Heating fluid inlet to the heat exchanger (T_{in}^h)	3.0
Heating fluid outlet from the heat exchanger (T_{out}^h)	1.0
Coolant fluid outlet from the heat exchanger (T_{out}^c)	0.8
Heating fluid inlet to the boiler (T_{in}^b)	1.5

The obtained average accuracies of mapping the temperature courses in the analysed nodes of the installation do not exceed 3 °C. The highest value of the mapping error occurs at the inlet of the heating fluid to the heat exchanger, i.e. behind the heat accumulator. As can be seen in Fig. 7, in this node the recorded increase in the temperature of the heating fluid is much faster than that resulting from the simulation calculations, which is related to the simplification used in the model. It was assumed that the heating fluid flowing into the heat accumulator will completely replace the fluid already in the heat accumulator before it flows to the next element of the installation.

4. CONCLUSIONS

The paper presents an original method of modelling the operation of a heat exchange installation for randomly changing temperatures. Accumulation elements with lumped parameters were used in the model of the heat exchange installation. The proposed approach is aimed at

facilitating the definition of model parameters and carrying out calculations of the installation at the design stage, with the prospect of frequent changes in its configuration. The paper presents an original model of the heat accumulating element, which takes into account the possibility of heat transfer from the heating medium to the walls and to the cooling medium or the environment. The process of heat accumulation and heat transport is described by means of three balance equations, with the parameters of the heating fluid, wall, and cooling agent defined by one mass, temperature, specific heat, etc.

Due to the assumed random-variable nature of the applied boundary conditions, the non-linear nature of the used in the calculation model of the function, the iterative calculation procedure of the accumulation element was used in the calculations. It enables flexible definition of temperatures of heating and cooling agents flowing into the installation, as well as their flow directions and properties. The applied method also enables the analysis of installations using control elements. Boundary conditions in heat accumulating elements are also defined in an original way. It has been proposed that the temperature at the inlet to the heat accumulating element should be corrected, taking into account the refilling the chamber of the heat accumulating element with a medium of changed temperature. It was assumed that when the refilling process is finished, the changed boundary conditions cover the entire heat accumulating element. The validation process of the proposed computational model of the accumulation element with lumped parameters was carried out for a water installation consisting of an upper heat source (boiler), a lower heat source (cooling water tank), a heat accumulator, a heat exchanger in which heat is transported from the heating medium to the cooling medium and pumps, three-way valve and pipelines. The obtained results allowed to conclude that the use of the computational model of the accumulation element with lumped parameters allows for a very good representation of the analysed heating process of the installation. The RMSE for the analysed points of the installation ranged from 1 °C to 3 °C. This result was obtained with a relatively small amount of work related to the construction of the computational model, also the model parameters used are few and easy to define at the initial design stage of the installation.

The structure of the model does not influence the frequencies at which it is working properly. Increasing the frequency of applied changes automatically changes the calculative time step. Another problem is the possibility of comparing the obtained results with experimental data, because the time lag of the thermocouples, which is defined using a time constant, is approximately 1 s for typical thermocouples (Oliveira, 2022). This means, that analyzing phenomena with a time step smaller than 0.1 s has no practical value. In the developed model,

it is also possible to randomly modify the external conditions of the analysed system (e.g. temperature of the ambient air), as well as the parameters of the process fluids. The developed model is to be used as a digital twin in the control of thermal processes occurring in a chemical installation. In particular, at the design stage, using this model it will be possible to work out alarm thresholds at which the installation operation mode will be switched to another mode or turned off.

ACKNOWLEDGMENTS

This research was co-funded by the National Centre of Research and Development and ORLEN SA in the EU Smart Growth Operational Programme, grant number POIR.04.01.01-00-0064/18-00.

SYMBOLS

A - heat transfer surface, m^2

c_c - specific heat of the cooling medium, $J/(kg \cdot K)$

c_h - specific heat of the heating medium, $J/(kg \cdot K)$

c_p - specific heat, $J/(kg \cdot K)$

c_w - specific heat of the wall, $J/(kg \cdot K)$

k - computational step, -

k_{max} - number of points in the analysed series, -

k_{ch}^h - number of points in the analysed series for heating medium, -

k_{ch}^c - number of points in the analysed series for heating medium, -

\dot{m} - mass flow rate, kg/s

m_c - mass of the cooling medium in the heat exchanger, kg

\dot{m}_c - mass flow rate of the cooling medium in the heat exchanger, kg/s

\dot{m}_{ch}^c - mass flow rate of the cooling medium, kg/s

\dot{m}_{ch}^h - mass flow rate of the heating medium, kg/s

m_h - mass of the heating medium in the heat exchanger, kg

\dot{m}_h - mass flow rate of the heating medium in the heat exchanger, kg/s

m_w - mass of the wall, kg

Q - heat flux, W

Q_{acc}^c - heat accumulated in the cooling medium, W

Q_{acc}^h - heat accumulated in the heating medium, W
 Q_{acc}^w - heat accumulated in the heat exchanger wall, W
 Q_{in}^c - heat flux delivered by the cooling medium, W
 Q_{in}^h - heat flux delivered by the heating medium, W
 Q_{out}^c - heat flux discharged by the cooling medium, W
 Q_{out}^h - heat flux discharged by the heating medium, W
 Q_{α}^c - heat flux transferred between the wall and the cooling medium, W
 Q_{α}^h - heat flux transferred between the heating medium and the wall, W
 T_{acc} - the heating fluid at the inlet to the heat accumulator (Acc), K
 T_{in}^b - temperature of the heating fluid at the inlet to the boiler (BO), K
 T_{out}^b - temperature of the heating fluid at the outlet of the boiler (BO), K
 T_{in}^c - temperature of the cooling fluid at the inlet to the heat exchanger (HE), K
 T_{out}^c - temperature of the coolant at the outlet of the heat exchanger (HE), K
 T_{in}^h - temperature of the heating fluid at the inlet to the heat exchanger (HE), K
 T_{out}^h - temperature of the heating fluid at the outlet of the heat exchanger (HE), K
 T_k^{exp} - temperature measured in the experiment, K
 t_w - temperature of the wall, K
 $t_{av_end}^h$ - average temperature of the heating medium in the heat exchanger in the current computational step, K
 $t_{av_ini}^h = t_w(k - 1)$ - average temperature of the heating medium in the heat exchanger during the previous computational step, K
 $t_{av_end}^c = t_w(k)$ - average temperature of the cooling medium in the heat exchanger in the current computational step, K
 $t_{av_ini}^c$ - average temperature of the cooling medium in the heat exchanger during the previous computational step, K
 $t_{av_end}^w$ - average temperature of the wall in the current computational step, K
 $t_{av_ini}^w$ - average temperature of the wall during the previous computational step, K
 t_{in}^c - inlet temperature of the cooling medium, K
 t_k^{sym} - calculated temperature, K
 t_{sup}^c - supply temperature of the cooling medium delivered by the pipe system, K
 t_{in}^h - inlet temperature of the heating medium, K
 t_{out}^c - outlet temperature of the cooling medium, K

t_{out}^h - outlet temperature of the heating medium, K

t_{ref}^h - reference temperature, K

t_{sup}^h - supply temperature of the heating medium delivered by the pipe system, K

V_{ch}^c - volume of the cooling chamber, m³

V_{ch}^h - volume of the heating chamber, m³

Greek symbols

α_c - heat transfer coefficient for the cooling medium, W/(m²·K)

α_h - heat transfer coefficient for the heating medium, W/(m²·K)

Δt - temperature difference, K

Δt_{av}^w - change of the average temperature of the wall over the computational time step, K

Δt_{h_w} - temperature difference between the heating medium and the wall, K

Δt_{w_c} - temperature difference between the wall and the cooling medium, K

Δt_{av}^c - change of the average temperature of the cooling medium over the computational time step, K

Δt_{av}^h - change of the average temperature of the heating medium over the computational time step, K

$\Delta \tau$ - computational time step, s

ρ_{ch}^c - average density of the cooling medium in the chamber, kg/m³

ρ_{ch}^h - average density of the heating medium in the chamber, kg/m³

τ - current time of the process, s

τ_{ch}^h - chamber refilling time for heating medium, s

τ_{ch}^c - chamber refilling time for cooling medium, s

τ_0 - initial time, s

Subscripts

ini - previous calculation step

end - current calculation step

Abbreviations

ANN - artificial neural network

CFD - computational fluid dynamics

CVP - control vector parameterization

EPSQP - external penalty sequential quadratic programming

GA - genetic algorithms

LMTD - logarithmic mean temperature difference

NSGA - non-dominated sequencing genetic algorithm

NTU - efficiency-number of heat-transfer units

PSO - particle swarm optimization

RMSE - the mean square error of the temperature

SQP - sequential quadratic programming

SVR - support vector machine regression

TOPSIS - technique for order of preference by similarity to ideal solution

REFERENCES

1. Alsanousie A.A., Elsamni O.A., Attia A.E., Elhelw M., 2021. Transient and troubleshoots management of aged small-scale steam power plants using Aspen Plus Dynamics. *Energy*, 223, 120079. DOI: [10.1016/j.energy.2021.120079](https://doi.org/10.1016/j.energy.2021.120079).
2. Aminmahalati A., Fazlali A., Safikhani H., 2021. Multi-objective optimization of CO boiler combustion chamber in the RFCC unit using NSGA II algorithm. *Energy*, 221, 119859. DOI: [10.1016/j.energy.2021.119859](https://doi.org/10.1016/j.energy.2021.119859).
3. Barone G., Buonomano A., Forzano C., Palombo A., 2020. A novel dynamic simulation model for the thermo-economic analysis and optimisation of district heating systems. *Energy Convers. Manage.*, 220, 113052. DOI: [10.1016/j.enconman.2020.113052](https://doi.org/10.1016/j.enconman.2020.113052).
4. Bhutta M.M.A., Hayat N., Bashir M.H., Khan A.R., Ahmad K.N., Khan S., 2012. CFD applications in various heat exchangers design: a review. *Appl. Therm. Eng.*, 32, 1–12. DOI: [10.1016/j.applthermaleng.2011.09.001](https://doi.org/10.1016/j.applthermaleng.2011.09.001).
5. Bird T.J., Jain N., 2020. Dynamic modelling and validation of a micro-combined heat and power system with integrated thermal energy storage. *Appl. Energy*, 271, 114955. DOI: [10.1016/j.apenergy.2020.114955](https://doi.org/10.1016/j.apenergy.2020.114955).
6. Brown D.M., Bhatt B.L., Hsiung T.H., Lewnard J.J., Waller F.J., 1991. Novel technology for the synthesis of dimethyl ether from syngas. *Catal. Today*, 8, 279–304. DOI: [10.1016/0920-5861\(91\)80055-E](https://doi.org/10.1016/0920-5861(91)80055-E).
7. Dahash A., Mieck S., Ochs F., Krautz H.J., 2019. A comparative study of two simulation tools for the technical feasibility in terms of modelling district heating systems: an optimization case study. *Simul. Modell. Pract. Theory*, 91, 48–68. DOI: [10.1016/j.simpat.2018.11.008](https://doi.org/10.1016/j.simpat.2018.11.008).

8. Dehghan A.A., Barzegar A., 2011. Thermal performance behaviour of a domestic hot water solar storage tank during consumption operation. *Energy Convers. Manage.*, 52, 468–476. DOI: [10.1016/j.enconman.2010.06.075](https://doi.org/10.1016/j.enconman.2010.06.075).
9. El-Azab H.-A.I., Swief R.A., El-Amarty N.H., Temraz H.K., 2018. Unit commitment towards decarbonized network facing fixed and stochastic resources applying water cycle optimization. *Energies*, 11, 1140. DOI: [10.3390/en11051140](https://doi.org/10.3390/en11051140).
10. Gabrielaitiene I., Bøhm B., Sunden B., 2007. Modelling temperature dynamics of a district heating system in Naestved, Denmark – a case study. *Energy Convers. Manage.*, 48, 78–86. DOI: [10.1016/j.enconman.2006.05.011](https://doi.org/10.1016/j.enconman.2006.05.011).
11. Gao H., Liu Y., Song X., Zheng B., Sun P., Lu M., Ma Y., Gao Z., 2019. Numerical study of heat transfer characteristics of semi-coke and steam in waste heat recovery steam generator for hydrogen production. *Int. J. Hydrogen Energy*, 44, 25160–25168. DOI: [10.1016/j.ijhydene.2019.05.155](https://doi.org/10.1016/j.ijhydene.2019.05.155).
12. Giraud L., Merabet M., Baviere R., Vallée M., 2017. Optimal control of district heating systems using dynamic simulation and mixed integer linear programming. *Proceedings of the 12th International Modelica Conference*, Prague, Czech Republic, 15–17 March 2017, 141–150. DOI: [10.3384/ecp17132141](https://doi.org/10.3384/ecp17132141).
13. Han Y., Sun Y., Wu J., 2020. An efficient solar/lignite hybrid power generation system based on solar-driven waste heat recovery and energy cascade utilization in lignite pre-drying. *Energy Convers. Manage.*, 205, 112406. DOI: [10.1016/j.enconman.2019.112406](https://doi.org/10.1016/j.enconman.2019.112406).
14. Jiang B., Xia D., Guo H., Xiao L., Qu H., Liu X., 2019. Efficient waste heat recovery system for high-temperature solid particles based on heat transfer enhancement. *Appl. Therm. Eng.*, 155, 166–174. DOI: [10.1016/j.applthermaleng.2019.03.101](https://doi.org/10.1016/j.applthermaleng.2019.03.101).
15. Kamal R., Moloney F., Wickramaratne C., Narasimhan A., Goswami D.Y., 2019. Strategic control and cost optimization of thermal energy storage in buildings using EnergyPlus. *Appl. Energy*, 246, 77–90. DOI: [10.1016/j.apenergy.2019.04.017](https://doi.org/10.1016/j.apenergy.2019.04.017).
16. Kang J.O., Kim S.C., 2019. Heat transfer characteristics of heat exchangers for waste heat recovery from a billet casting process. *Energies*, 12, 2695. DOI: [10.3390/en12142695](https://doi.org/10.3390/en12142695).
17. Kluba A., Field R., 2019. Optimization and exergy analysis of nuclear heat storage and recovery. *Energies*, 12, 4205. DOI: [10.3390/en12214205](https://doi.org/10.3390/en12214205).
18. Knabner P., Angermann L., 2003. *Numerical methods for elliptic and parabolic partial differential equations*. Springer, New York, 7–13. DOI: [10.1007/b97419](https://doi.org/10.1007/b97419).

19. Kropiwnicki J., Furmanek M., Rogala A., 2021. Modular approach for modelling warming up process in water installations with flow-regulating elements. *Energies*, 14, 4599. DOI: [10.3390/en14154599](https://doi.org/10.3390/en14154599).
20. Kuang J., Zhang C., Li F., Sun B., 2018. Dynamic optimization of combined cooling, heating, and power systems with energy storage units. *Energies*, 11, 2288. DOI: [10.3390/en11092288](https://doi.org/10.3390/en11092288).
21. Li S., Deng Z., Liu J., Liu D., 2022. Multi-objective optimization of plate-fin heat exchangers via non-dominated sequencing genetic algorithm (NSGA-II). *Appl. Sci.*, 12, 11792. DOI: [10.3390/app122211792](https://doi.org/10.3390/app122211792).
22. Li D., Wang J., Ding Y., Yao H., Huang Y., 2019. Dynamic thermal management for industrial waste heat recovery based on phase change material thermal storage. *Appl. Energy*, 236, 1168–1182. DOI: [10.1016/j.apenergy.2018.12.040](https://doi.org/10.1016/j.apenergy.2018.12.040).
23. Li P., Wang H., Lv Q., Li W., 2017. Combined heat and power dispatch considering heat storage of both buildings and pipelines in district heating system for wind power integration. *Energies*, 10, 893. DOI: [10.3390/en10070893](https://doi.org/10.3390/en10070893).
24. Oliveira A.V.S., Avrit A., Gradeck M., 2022. Thermocouple response time estimation and temperature signal correction for an accurate heat flux calculation in inverse heat conduction problems. *Int. J. Heat Mass Transfer*, 185, 122398. DOI: [10.1016/j.ijheatmasstransfer.2021.122398](https://doi.org/10.1016/j.ijheatmasstransfer.2021.122398).
25. Oppelt T., Urbaneck T., Gross U., Platzer B., 2016. Dynamic thermo-hydraulic model of district cooling networks. *Appl. Therm. Eng.*, 102, 336–345. DOI: [10.1016/j.applthermaleng.2016.03.168](https://doi.org/10.1016/j.applthermaleng.2016.03.168).
26. Pal E., Kumar I., Joshi J.B., Maheshwari N.K., 2016. CFD simulations of shell-side flow in a shell-and-tube type heat exchanger with and without baffles. *Chem. Eng. Sci.*, 143, 314–340. DOI: [10.1016/j.ces.2016.01.011](https://doi.org/10.1016/j.ces.2016.01.011).
27. Pudlik W., 2012. *Wymiana i wymienniki ciepła*. Wydawnictwo Politechniki Gdańskiej, 143. Available at: <https://press.pg.edu.pl/book/428>.
28. Shi Y., Zhong W., Chen X., Yu A.B., Li J., 2019. Combustion optimization of ultrasupercritical boiler based on artificial intelligence. *Energy*, 170, 804–817. DOI: [10.1016/j.energy.2018.12.172](https://doi.org/10.1016/j.energy.2018.12.172).
29. Shu J., Fu J., Ren C., Liu J., Wang S., Feng S., 2020. Numerical investigation on flow and heat transfer processes of novel methanol cracking device for internal combustion engine exhaust heat recovery. *Energy*, 195, 116954. DOI: [10.1016/j.energy.2020.116954](https://doi.org/10.1016/j.energy.2020.116954).

30. Skoglund T., Årzén K.-E., Dejmeek P., 2006. Dynamic object-oriented heat exchanger models for simulation of fluid property transitions. *Int. J. Heat Mass Transfer*, 49, 2291–2303. DOI: [10.1016/j.ijheatmasstransfer.2005.12.005](https://doi.org/10.1016/j.ijheatmasstransfer.2005.12.005).
31. Sobczak J., Wysocka I., Murgrabia S., Rogala A., 2022. A review on deactivation and regeneration of catalysts for dimethyl ether synthesis. *Energies*, 15, 5420. DOI: [10.3390/en15155420](https://doi.org/10.3390/en15155420).
32. Vesterlund M., Dahl J., 2015. A method for the simulation and optimization of district heating systems with meshed networks. *Energy Convers. Manage.*, 89, 555–567. DOI: [10.1016/j.enconman.2014.10.002](https://doi.org/10.1016/j.enconman.2014.10.002).
33. Wang J., Bian H., Cao X., Ding M., 2021. Numerical performance analysis of a novel shell-and-tube oil cooler with wire-wound and crescent baffles. *Appl. Therm. Eng.*, 184, 116298. DOI: [10.1016/j.applthermaleng.2020.116298](https://doi.org/10.1016/j.applthermaleng.2020.116298).
34. Wysocka I., Hupka J., Rogala A., 2019. Catalytic activity of nickel and ruthenium–nickel catalysts supported on SiO₂, ZrO₂, Al₂O₃, and MgAl₂O₄ in a dry reforming process. *Catalysts*, 9, 540. DOI: [10.3390/catal9060540](https://doi.org/10.3390/catal9060540).
35. Yusuf A., Bayhan N., Tiryaki H., Hamawandi B., Toprak M.S., Ballikaya S., 2021. Multi-objective optimization of concentrated Photovoltaic-Thermoelectric hybrid system via non-dominated sorting genetic algorithm (NSGA II). *Energy Convers. Manage.*, 236, 114065. DOI: [10.1016/j.enconman.2021.114065](https://doi.org/10.1016/j.enconman.2021.114065).
36. Zheng T., Zhao Li.-P., 2022a. Dynamic flow optimization for a three-loop fluid heat dissipation system in spacecraft. *Case Stud. Therm. Eng.*, 40, 102496. DOI: [10.1016/j.csite.2022.102496](https://doi.org/10.1016/j.csite.2022.102496).
37. Zheng T., Zhao Li.-P., 2022b. Dynamic optimization analyses and algorithm design for the parallel heat exchange system in spacecraft. *Appl. Therm. Eng.*, 212, 118519. DOI: [10.1016/j.applthermaleng.2022.118519](https://doi.org/10.1016/j.applthermaleng.2022.118519).
38. Zhou H., Xinping Q., Kefa C., Fan J., 2004. Optimizing pulverized coal combustion performance based on ANN and GA. *Fuel Process. Technol.*, 85, 113–124. DOI: [10.1016/S0378-3820\(03\)00155-3](https://doi.org/10.1016/S0378-3820(03)00155-3).